Small-angle neutron scattering studies of molecular clustering in mixtures of polyethylene and deuterated polyethylene

J. Schelten,
Institüt für Festkorperforschung, Kernforschungsanlage, Julich 1, Postfach 365, W. Germany
and G. D. Wignall,
ICI Europa Ltd, Everslaan 45, B 3078 Everberg, Belgium
and D. G. H. Ballard and G. W. Longman
ICI Corporate Laboratory, The Heath, Runcorn WA7A QE, UK
(Received 4 July 1977)

Studies of the factors governing molecular aggregation in mixed samples of protonated polyethylene (PEH) and deuterated polyethylene (PED) have been made by small-angle neutron scattering. Thermodynamic arguments are given to show that there is a natural tendency for PEH and PED to segregate on crystallizing from the melt. This segregation arises from the shape of the phase diagram of the PEH/PED system, and not from any basic incompatibility of the components. An equilibrium distribution of PED molecules in PEH can be obtained only by cooling very rapidly and quenching in the equilibrium distribution of the melt, or alternatively by cooling extremely slowly, giving the molecules sufficient time to rearrange to a statistical distribution. Because of the very low diffusion rates of the polymer molecules ($M_w \sim 100\,000$), the rates of cooling normally used in practice ($>2^\circ$C/h) are not sufficiently slow to reach an equilibrium distribution and non-equilibrium crystallization produces partly segregated or clustered distributions. By means of careful control of the cooling rate on crystallization, the molecular weights, concentrations and melting points of the two species, it is possible to prepare samples covering the whole range from virtually phase separated to statistically mixed molecules. Departures from a statistical distribution lead to anomalous features in the SANS patterns, and these features have been used to study the aggregation (clustering) process. Model calculations of the scattering patterns from clustered molecules have been performed which explain all the anomalous features detected in the SANS patterns. These calculations show that the SANS method is extremely sensitive to small deviations from a statistical distribution. The model calculations also provide important indirect evidence that the radius of gyration of the polymer molecule is virtually unchanged on equilibrium crystallization from the unperturbed dimensions measured in the melt.

INTRODUCTION

In recent years the small-angle neutron scattering (SANS) method has been developed into a powerful technique for the study of chain conformation in bulk polymers[1–8] and copolymers[9]. Samples analysed by this method are made up of a host polymer matrix in which a small number of isotopically substituted polymer molecules (tagged molecules) are dispersed. Samples may be made with a protonated matrix and deuterated tagged molecules[8], or vice versa[2]. The measured scattering parameters are in principle the same, and the choice of matrix is usually determined by experimental considerations (availability of characterized deuterated polymer, level of background incoherent scattering, sample thickness and transmission etc.).

A fundamental assumption upon which the scattering theory is based is that the tagged molecules are randomly or statistically dispersed in the host matrix and scatter incoherently with respect to each other[3]. Any departure from a statistical distribution, either by way of aggregation of the tagged molecules, or correlations of their positions and trajectories, invalidates the scattering theory and makes the interpretation of the scattering increasingly uncertain.

It was pointed out by Stehling, Ergos and Mandelkern[10] that PEH and PED had a melting point difference of ~6°C, and the conclusion drawn from a series of thermodynamic studies was that a statistical dispersion of tagged molecules in the matrix could not be assumed. An extreme case of a non-statistical distribution would be the case of phase segregation of PEH and PED, though there is a whole range of aggregation possibilities which fall short of complete phase segregation. For example in crystals of the same overall composition one might observe fluctuations in the distribution of the dispersed tagged molecules. This might arise if one or more molecules crystallized with a correlation of the molecular centres of gravity and trajectories, to form a cluster of tagged molecules. It is such a concept of a cluster which we first proposed to explain anomalous molecular weights observed via SANS in mixtures of protonated polyethylene and deuterated polyethylene[3–5]. Because of the importance of potential deviations from a statistical distribution on the interpretation of SANS and infra-red studies of chain configuration[11–13], we have continued our studies of this problem, and present in this paper our accumulated experience on the factors governing the achievement of a statistical distribution of tagged molecules in mixed PEH–PED systems.

We have also performed model calculations of the scattering patterns associated with clusters, which show that this hypothesis can explain not only the anomalies in molecular weight (Σ_0) and radius of gyration (R_g) of the tagged molecules, but also the general shape of the scattering curves in both the low ($0.002 \leqslant K \leqslant 0.02$ Å^{-1}) and intermediate ($0.02 \leqslant K \leqslant 0.2$ Å^{-1}) ranges of $K = (4\pi/\lambda)\sin\theta$. However, before performing these calculations, we had not appreciated the extreme sensitivity of the SANS technique to very small departures from the statistical distribution. The term cluster suggests a physical aggregate of tagged molecules, implying substantial correlations of the molecular centres of gravity and trajectories, and it was in this sense we had first introduced the term. As a result of our model calculations it is now appreciated that such large departures from randomness are not necessarily implied by SANS anomalies in Σ_0 and R_g. Very minor departures from a statistical distribution involving as few as one in one thousand nearest neighbour units for a given molecule are sufficient to cause substantial anomalies in Σ_0 and R_g. For this reason we wish to modify the term 'cluster' and suggest the term 'paracluster' for these minor deviations. The latter term is meant to stress that very minor deviations from a statistical distribution are sufficient to cause anomalies in Σ_0 and R_g and that gross physical aggregation of tagged molecules is not necessarily implied by these anomalies. This better appreciation of the extreme sensitivity of the SANS technique to minor deviations from a statistical distribution, reinforces our original point that unambiguous conclusions can only be drawn from SANS data showing no artefacts from paraclustering effects.

SANS STUDIES

It is well known that the extrapolated forward scattering cross-section of the tagged molecules is a measure of their weight-averaged molecular weight, Σ_0 which is given by[1–5,8]:

$$1/\Sigma_0 = (1/cK_N)(d\Sigma/d\Omega)_{K=0} \qquad (1)$$

where c is the concentration of tagged molecules, K_N is a calibration constant[3,4,8] and $d\Sigma(K)/d\Omega$ is the differential scattering cross-section of the molecules as a function of $K = (4\pi/\lambda)\sin\theta$. λ is the neutron wavelength and 2θ the usual angle of scatter. $(d\Sigma/d\Omega)_{K=0}$ is obtained from plots of $(1/d\Sigma/d\Omega)$ *versus* K^2 which are linear at low K. The slope of such plots yields the radius of gyration, $R_g = \langle S^2\rangle 1/2$, of the polymer molecule for a statistical distribution of tagged molecules.

FACTORS GOVERNING THE PARACLUSTERING PHENOMENON

The internal self consistency of the data may be checked by comparing values of Σ_0 obtained from equation (1) with calues of M_w, the weight-averaged molecular weights obtained by g.p.c. techniques prior to blending. Where the two values are equal within the total experimental error (∓20%) it is reasonable to assume that a statistical distribution of tagged molecules has been achieved and such agreement has been found generally for amorphous polymers[1,2]. In the case of semicrystalline polymers, however, initial experiments showed that molecular weights measured by neutron scattering could by systematically higher than those measured by g.p.c. by a factor exceeding the combined errors by many times[3]. This is illustrated in *Table 1* which shows that for samples blended in *ortho*-dichlorobenzene (ODCB) the neutron and g.p.c. molecular weights are in reasonable agreement. However for samples blended in xylene, Σ_0 can exceed M_w by ~15 times. Presumably the reason for this discrepancy is the higher boiling point of ODCB (~180°C) compared to ~140°C for xylene, which gives a more complete dissolution of the PEH (melting point ~135°C) and PED (melting point ~129°C) in the solution. It may also be seen from *Table 1* that as the apparent molecular weight Σ_0 exceeds M_w the apparent radius of gyration of the scattering entity exceeds that of the single molecule. In both cases the polymer was precipitated from solution into a non-solvent (methanol) and the resultant powders were dried in a vacuum oven at 70°C and subsequently compression moulded at 190°C into a form suitable for neutron measurements (~1 mm thick). After compression moulding, the samples were rapidly quenched into water (~10°C).

The measurements shown in *Table 1*, were taken at 25°C, and subsequently measurements were made in the melt at 150°C[3,8]. These showed that for unclustered samples blended in ODCB, melting produced no segregation, and measurements over periods of several hours showed agreement between Σ_0 and M_w. For samples blended in xylene it was observed that on melting the large mismatch between Σ_0 and M_w (*Table 1*) gradually disappeared over periods of several hours in the melt[3]. It appears therefore that the equilibrium distribution in the melt is statistical, though long time periods may be needed to reach equilibrium. This statistical distribution can be quenched into the solid state by means of sufficiently rapid cooling of the samples[8], and it was for this reason that samples were quenched into water after compression moulding. For clustered samples blended in xylene, the period of melt pressing (~4 min) was evidently not sufficient to disperse the tagged molecules and achieve a statistical distribution, and it appears that a non-statistical distribution of tagged molecules must already have been present in the powders precipitated from xylene into methanol. It will be seen in subsequent sections that even where samples have a statistical distribution in the melt, a non-statistical distribution can again arise in the solid if the samples are crystallized by slow cooling.

Table 2 shows the effect of a mismatch in molecular weight between the matrix and the tagged molecules. It may be seen that when the molecular weights of the matrix and tagged molecules are approximately matched, no clustering effects occur for quenched samples, as evidenced by the agreement between Σ_0 and M_w. However when there is a large mismatch in the molecular weights of the matrix and the

Table 1 Weight-averaged molecular weights of tagged molecules from g.p.c. and small-angle neutron scattering

	Blended in *ortho*-dichlorobenzene (~180°C)	Blended in xylene (~138°C)
$\frac{\Sigma_0}{M_w} = \frac{\text{molecular weight (neutrons)}}{\text{molecular weight (g.p.c.)}}$	0.95 ∓ 0.1	15 ∓ 5
$\frac{R_g}{M_w^{1/2}} = \frac{\langle S^2\rangle_w^{1/2}}{M_w^{1/2}}$	0.46 ∓ 0.05	1.02 ∓ 0.1

All samples rapidly quenched from melt into water and measured at 25°C (concentration of tagged molecules ≤5%)

Table 2 Paraclustering effects in tagged molecules (PED) as a function of molecular weight. Matrix (PEH) has molecular weight ~100 000

Molecular weight of tagged molecules (g.p.c.), M_w	$\frac{\Sigma_0}{M_w} = \frac{\text{molecular weight (neutrons)}}{\text{molecular weight (g.p.c.)}}$	$\frac{R_g}{M_w^{1/2}} = \frac{\langle S^2 \rangle_w^{1/2}}{M_w^{1/2}}$
3000	73 ∓ 7	4.1
12 000	7 ∓ 1	1.8
60 000	0.91 ∓ 0.1	0.49
140 000	0.94 ∓ 0.1	0.42

All samples solution blended in *ortho*-dichlorobenzene quenched rapidly from the melt and measured at 25°C (concentration of tagged molecules ≤5%)

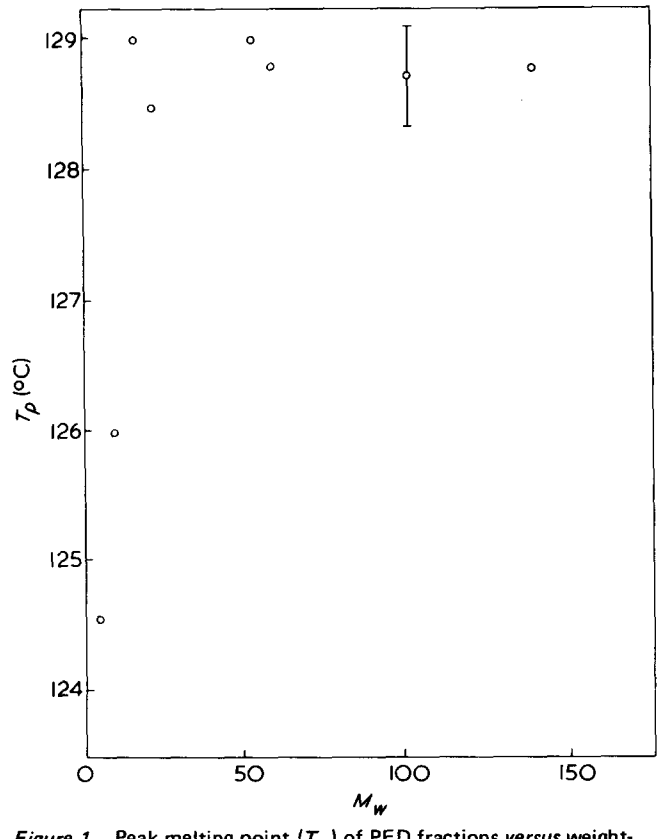

Figure 1 Peak melting point (T_p) of PED fractions *versus* weight-averaged molecular weight (M_w) of fractions. Samples crystallized from the melt at 0.62°C/min and remelted at 5°C/min, M_w/M_n = 1.85 ± 0.3

tagged molecules there is an increasing discrepancy between Σ_0 and M_w.

Figure 1 shows the melting points of the PED fractions as a function of molecular weight. The melting points are sensibly constant down to a molecular weight ~17 000 after which they fall rapidly to a value ~124.6°C at M_w = 4600. Under the same conditions of measurement the matrix has a melting point of 135°C.

The melt viscosities of polyethylene at 150°C are 0.6 poise (M_w = 3000), 87 poise (M_w = 12 000) and 2.6 × 10^3 poise (M_w = 60 000). Thus it appears that as long as the melt viscosity is high and the melting point gap is ~6°C no clustering takes place on quenching. As the molecular weight of the tagged molecules falls, both the mobility of the molecules, and the melting point gap increase, and the molecules again commence to cluster.

Table 3 shows the effect of the concentration of the tagged molecules on the clustering process. Where the molecular weights of the matrix are approximately matched there is no clustering as long as the concentration of tagged molecules ≤6% w/w. When the concentration of tagged molecules increases to 10%, clustering again occurs.

Because of the above evidence it was considered that a sample slow cooled from the melt would have a high probability of crystallizing with a non-random distribution of molecules in the solid state. For this reason an attempt was made to reduce this probability of clustering in slow cooled samples by choosing a slightly branched PEH polymer, whose thermal characteristics match those of the deutero-material. The temperatures for the start of crystallization, T_s, and peak crystallization rate, T_p, were T_s = 113.7°C, T_p = 111.7°C and T_s = 113.5°C, T_p = 112°C, for the PEH and PED materials, respectively. These materials were then solution blended in *ortho*-dichlorobenzene as described above, and slow cooled from the press at 1°C/min after compression moulding. It will be seen from *Table 3* that clustering still occurs in this type of sample as evidenced by the anomalously high values of Σ_0/M_w. Moreover Σ_0/M_w increases as the concentration of tagged molecules increases.

For all the samples described above and listed in *Tables 1–3* the matrix was unfractionated PEH with $M_w/M_N \sim 7$, and we were concerned to investigate the possibility that some or all of the anomalous molecular weights might originate from this wide distribution. One possible mechanism might plausibly lie in the known molecular weight dependence of the crystallization rate whereby the different components of the PEH matrix might crystallize selectively according to molecular weight. For this reason the PEH matrix was fractionated and a series of samples were made in which the PEH and PED molecules had approximately matched melting points, molecular weights and polydispersities. The molecular weights and thermal characteristics are shown in *Table 4*. These parameters were used to obtain the best overall match between the molecular weight, polydispersities, crystallization and melting temperatures of the PEH and PED components.

Table 5 shows the SANS results for this series of samples. After blending in ODCB and quenching after melt pressing, the results (*Table 5a*), show the higher molecular weight materials are unclustered, though there is a very slight tendency to clustering with the low molecular weight species (M_w = 17 000), presumably due to the increased mobility of the shorter molecules.

Table 3 Changes of tagged molecules (PED) with concentration and rate of cooling from the melt. The matrix has a molecular weight ~100 000

	Molecular weight (g.p.c.), M_w	Concentration, c (% w/w)	$\frac{\Sigma_0 \text{ (neutrons)}}{M_w \text{ (g.p.c.)}}$
Rapidly quenched samples	43 000	3	1.2
	60 000	3	0.9
	60 000	6	0.8
	140 000	3	1.0
	140 000	5	0.9
	140 000	10	2.4
Slowly cooled from melt at 1°C/min	60 000	3	5.7
	60 000	6	11.5

Table 4 Molecular weights and thermal characteristics of matched samples

	PEH matrix (slightly branched)					PED tagged molecules				
Sample no.	10^{-3} M_w	M_w/M_n	T_s cryst	T_p cryst	T_p melt	10^{-3} M_w	M_w/M_n	T_s cryst	T_p cryst	T_p melt
PE 31	217.0	1.66	116.8	114.0	125.0	510	2.40	118.0	116.1	127.0
PE 32	217.0	1.66	116.8	114.0	125.0	383	2.07	117.9	115.7	127.5
PE 33	89.9	1.39	119.8	116.3	125.8	102	1.52	119.4	116.6	128.7
PE 34	74.4	2.16	119.6	116.2	126.0	60	1.54	120.4	117.5	128.8
PE 35	41.5	2.13	120.3	118.7	127.0	54	1.63	120.5	118.1	129.0
PE 36	27.7	2.55	121.5	119.3	127.0	17	2.18	121.2	119.3	129.0
PE 37	15.7	1.94	121.0	119.0	127.0	17	2.18	121.2	119.3	129.0

T_s cryst is temperature for start of crystallisation from melt at 0.6–2°C/min; T_p cryst is peak crystallization temperature; T_p melt is peak melting point on subsequently remelting at 5°C/min

Table 5 SANS results for matched samples with different thermal histories

Sample no.	c (gm/gm)	10^{-3} M_w	Σ_0/M_w	R_g (Å)
(a) Quenched from the melt				
PE 31	0.031	510	0.99	399
PE 32	0.033	383	0.96	327
PE 33	0.051	102	1.36	208
PE 34	0.052	60	1.40	134
PE 35	0.053	54	1.00	131
PE 36	0.053	17	1.50	99
PE 37	0.051	17	1.80	100
(b) Slow cooled from melt at 0.1°C/min				
PE 31	0.031	510	15.5	1130
PE 32	0.033	383	15	1070
PE 34	0.052	60	170	979
PE 35	0.053	54	140	913
PE 36	0.053	17	909	1770
PE 37	0.051	17	721	2000
(c) Annealed at 123°C for 24 h				
PE 31	0.031	510	1.7	390
PE 32	0.033	383	2.9	359
PE 34	0.052	60	15.0	320
PE 35	0.053	54	7.4	200
PE 36	0.053	17	35.4	340
PE 37	0.051	17	188	816

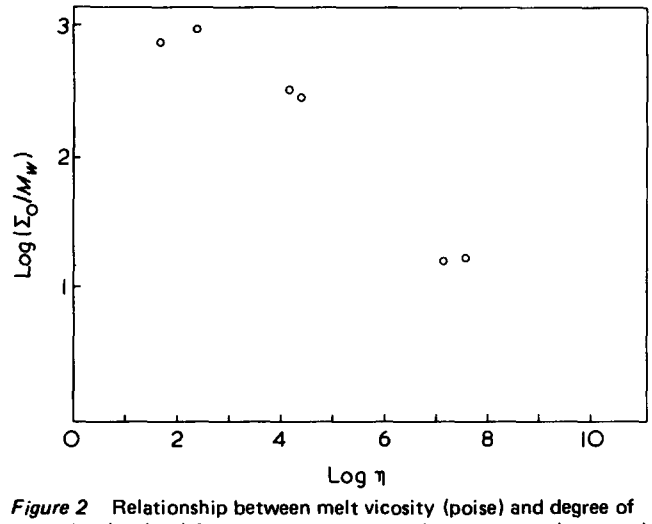

Figure 2 Relationship between melt vicosity (poise) and degree of clustering (Σ_0/M_w) for samples slow cooled from the melt (*Table 5b*)

On slow cooling the samples from the melt at 0.1°C/min, it is apparent that clustering takes place on a large scale and there is a marked correlation with molecular weight, with the higher molecular weight species showing the least clustering effects. *Figure 2* shows the relationship between the melt viscosity of the tagged molecules and the degree of clustering (Σ_0/M_w) for the data shown in *Table 5b*. Clustering increases with decreasing melt viscosity confirming that the mobility of the molecules is a controlling factor in the clustering process. A similar conclusion can be drawn from *Table 5c* showing data from samples annealed close to the melting point at 123°C for 24 h. Again the higher molecular weight species show low levels of clustering, though the samples become progressively more clustered as the molecular weight falls.

For this series of samples the annealing process results in approximately 60% of the original material in the sample being melted. It is apparent from the high molecular weight data showing small aggregation effects that annealing leaves the overall size of the molecules little changed. This is consistent with previous conclusions[8], that the radius of gyration is determined by the overall mass distribution of chain elements which are distributed over several lamellae. Hence on annealing the re-ordering process within the lamellae leaves the radius of gyration unchanged. When the molecules become sufficiently mobile to change their overall mass distribution, they simultaneously commence to cluster.

A final series of samples was measured to check these overall conclusions and the results are shown in *Table 6*. Samples PE 22–25 were originally prepared and measured in a previous paper[8], and for the present study the original quenched samples were annealed for selected times/temperatures as shown in *Table 6*. The broad conclusion that whenever the molecules have sufficient mobility to change their configuration, they will simultaneously commence to cluster is borne out. Where annealing allows the local order to increase, without allowing migration of the whole molecule, the radius of gyration is little changed.

The general conclusion from the above data is that in mixed PEH–PED systems, a statistical distribution of tagged molecules as measured by SANS, is the exception rather than the rule. Deviations from a statistical distribution can arise in the blending stage or in subsequent crystallization of the samples from the melt. These deviations increase with the mobility of the molecules, their concentration, the melting point difference of the two components and vary inversely with the speed of cooling from the melt. A statistical distribution as measured by SANS can only be achieved for small concentrations of tagged molecules (≤6%) of low mobility (M_w greater than ~60 000), which are rapidly quenched

Table 6 SANS results for samples annealed for different time/temperatures

Sample no.	10^{-3} M_w	M_w/M_n	Annealing conditions	Σ_0	Σ_0/M_w	R_g (Å)
PE 22	140	2.1	Quenched from melt	121	0.86	197
PE 22	140	2.1	Annealed at 124°C for 30 min	150	1.07	
PE 23	140	2.1	Quenched from melt	143	1.02	189
PE 23	140	2.1	Annealed at 124°C for 24 h	8161	583	700
PE 24	383	2.1	Quenched from melt	275	0.72	276
PE 24	383	2.1	Annealed at 119°C for 24 h	298	0.80	250
PE 25	54	2.1	Quenched from melt	58	1.07	142
PE 25	54	2.1	Annealed at 119°C for 30 min	70.4	1.3	124

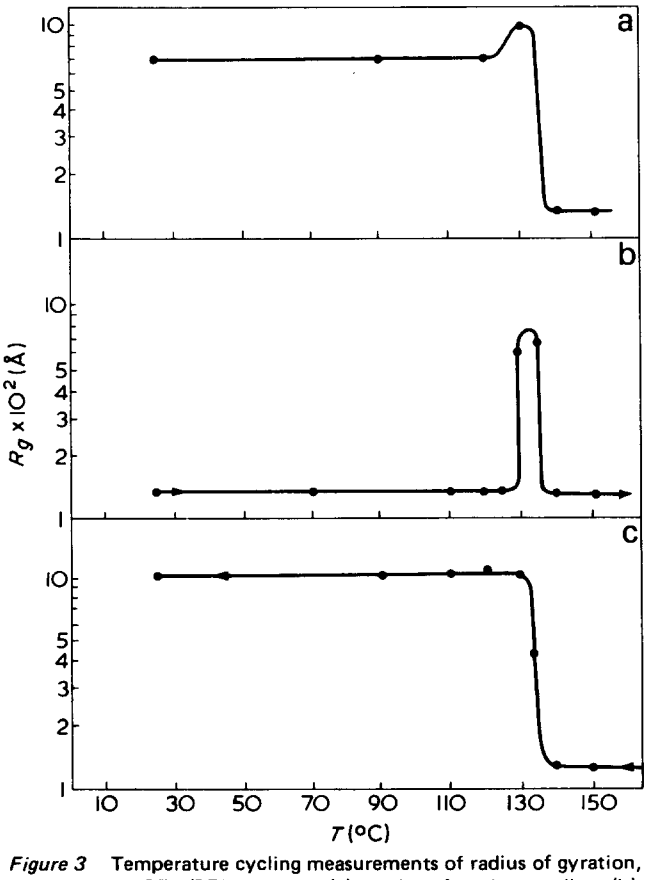

Figure 3 Temperature cycling measurements of radius of gyration, R_g, for mixed PEH/PED systems: (a) heating after slow cooling; (b) heating after quenching; (c) cooling from the melt

from the melt into ice–water on acetone/solid CO_2 mixtures. This suggests that there is a natural tendency of PEH and PED molecules to segregate, and that a statistical distribution can only be achieved by restricting the mobility and crystallization time so that separation of the molecules is avoided.

Clustering apparently takes place on solidification and hence one would expect the shape and positions of the liquidus and solidus boundaries of the phase diagram to play a crucial role in the clustering process. For this reason a series of temperature cycling studies was undertaken to map out the region where clustering originates. These studies are described below and confirm that clustering originates within the liquidus–solidus boundaries of the phase diagram. The thermodynamic considerations governing these boundaries are given below before going on to consider the paracluster model describing the SANS scattering patterns (see below)

TEMPERATURE CYCLING STUDIES

Figures 3a–c show temperature cycling studies for sample PE 25 (ref 8, Table 1). *Figure 3a* shows the value of R_g on reheating after initially slow-cooling from the melt. R_g remains constant on reheating until $T \sim 130$°C where it falls to a constant value in the melt. On quenching from the melt the value of R_g is unchanged (*Figure 3b*), confirming that the overall size distribution of the molecule is frozen in on a fast quench. On reheating R_g is constant until $T \sim 130$°C where it rises to large values indicating that the molecules are clustering in the range 130°–136°C. Thereafter R_g returns to its low equilibrium melt value. *Figure 4* shows typical low K plots of SANS data *versus* K^2, for the molten and quenched samples measured at 150° and 23°C, respectively. On measuring at $T = 132$°C some clustering of the molecules occurs: the plots are still linear with the same slope, but exhibit different values of R_g and Σ_0. On slow cooling from the melt (*Figure 3c*), clustering again commences at $T = 136$°C, and R_g rises to a high apparent value which is 'frozen', in the solid state at $T \sim 130$°C. The final value of R_g differs slightly from that shown in *Figure 3a* confirming that small variations in cooling rate affect the final degree of clustering. These experiments confirm that clustering arises in the rela-

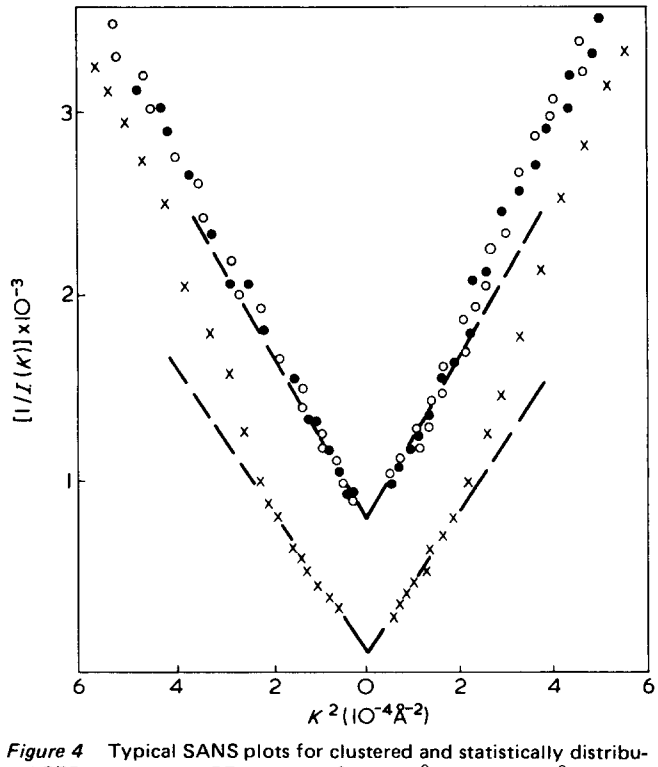

Figure 4 Typical SANS plots for clustered and statistically distributed PED molecules in PEH matrix: ●, $T = 23$°C; X, $T = 132$°C; ○, $T = 150$°C

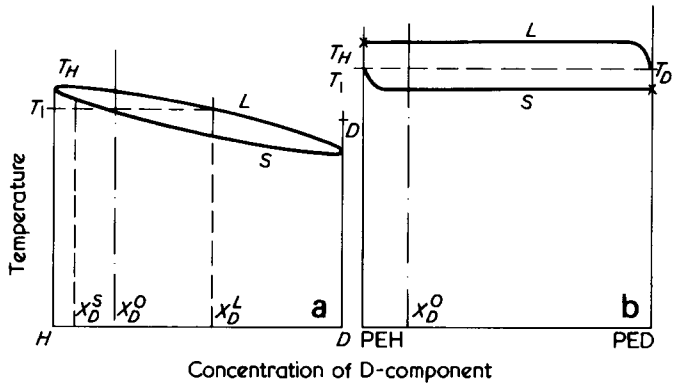

Figure 5 (a) Schematic explanation of symbols describing the phase diagram. (b) Schematic phase diagram for PEH/PED system

tively narrow temperature range 125°–135°C, that the melt distribution is statistical in equilibrium, and that either a statistical or non-statistical distribution can be frozen into the solid state. The thermodynamic considerations affecting the solidus–liquidus boundaries are given in the next section.

THERMODYNAMIC ASPECTS OF THE PHASE DIAGRAM OF PEH/PED SYSTEMS

To our knowledge the phase diagram is not known for this two-phase system consisting of the two H and D components. It is, however, known that the melting temperature of the PED is ~6°C less than that of PEH provided both components are unbranched polyethylene[10]. If we assume that the solution is ideal, i.e. there is no excess Gibbs free energy, one can calculate a solidus (S) and liquidus (L) line. The composition of the two phases at equilibrium can be calculated from the relations[14]:

$$\ln \frac{X_D^S}{X_D^L} = \frac{\Delta H_D}{R}\left(\frac{1}{T} - \frac{1}{T_D}\right) \tag{2}$$

$$\ln\left(\frac{1 - X_D^S}{1 - X_D^L}\right) = \frac{\Delta H_H}{R}\left(\frac{1}{T} - \frac{1}{H}\right) \tag{3}$$

The meaning of the symbols is given schematically in *Figure 5*, where ΔH_D and ΔH_H are the molar heats of fusion of the D and H components.

Let us assume that the two latent heats are the same; in this case and we obtain:

$$X_D^S/X_D^L = \frac{1 - X_D^L}{1 - X_D^S} = K_1 \tag{4}$$

$$K_1 = \exp\left[\frac{\Delta H}{R}\left(\frac{1}{T_H} - \frac{1}{T_D}\right)\right] \tag{5}$$

Using the literature value of $\Delta H = 66.4$ cal/g for linear polyethylene[15], $T_D = 402$K, and $T_H = 408$K and $M = 100\,000$ g gives:

$$K_1 = \exp(-122) \approx 0 \tag{6}$$

With this small value the solidus and liquidus line form the rectangle as shown in *Figure 5b*. Furthermore this shape is not significantly changed if one takes into account the fact that ΔH_H and ΔH_D are different but of the same order of magnitude. Mathematically, this strange shape is caused by the fact that for high molecular weight the molar latent heat is much larger than RT_H. The physics behind this is, however, that the entropy of mixing of polymer molecules is small. It is given by

$$\Delta S_{mix} = k_B(N_H \ln n_H + N_D \ln n_D) \tag{7}$$

where n_H and n_D are the mole fractions, and N_H and N_D are the number of polymer molecules of both components. One sees that the specific entropy is inversely proportional to the molecular weight, and it becomes very small for large molecular weight polymer molecules.

With such a phase diagram one can readily understand how phase separation can occur when the polymer is solidified. Certainly, phase separation is almost complete in equilibrium at a temperature T_1 as shown in *Figure 5*. If non-equilibrium solidification occurs, the phase separation at T_1 will not be complete neither will a solid solution be obtained at temperatures below the solidus line. However, at temperatures between the liquidus and the solidus lines phase separation can take place at least partly. This separation can be predicted to increase with the temperature difference $T_H - T_D$, higher concentration of tagged molecules, slower cooling rates from the melt and higher mobility of the polymer molecules. Thus the hypothesis that clusters arise because of the tendency of PEH and PED molecules to phase separate, when crystallized from the statistical distribution of the melt, can easily explain the general features of the data given above.

If the molecules have the appropriate cooling rate and mobility, almost complete phase separation is to be expected, and this has been demonstrated for some samples (see ref 8, figure 2). However, the thermodynamic assumptions and arguments given above indicate that with infinitely slow cooling, the molecules should again be statistically distributed.

Similarly, annealing for long periods in the solid state below the solidus boundary should in principle produce a statistically distributed system. However, due to the extremely low diffusion coefficients of polymer molecules in the solid state, it has not been found possible in practice to use these methods to produce statistically distributed molecules. In order to produce any change in R_g or Σ_0 by annealing over periods ~1 – 2 days, it was found necessary to choose a temperature which partly melted the sample, leading to clustering. Thus the only practical way to making statistically distributed molecules has been to work with relatively rapid quench rates.

It will be seen from the subsequent discussion that most of the data given above, with relatively fast quench rates and low degrees of clustering ($\Sigma_0/M_w < 1000$), can be explained by relatively minor deviations from a statistical distribution. It is for these kinds of deviations the term paracluster is appropriate.

SCATTERING FUNCTION FROM CLUSTERED MOLECULES: THE PARACLUSTER MODEL

As explained above the experimental observation that forward scattering and radius of gyration are larger than for a statistical distribution of tagged molecules, had suggested that regions were formed which were depleted of tagged molecules.

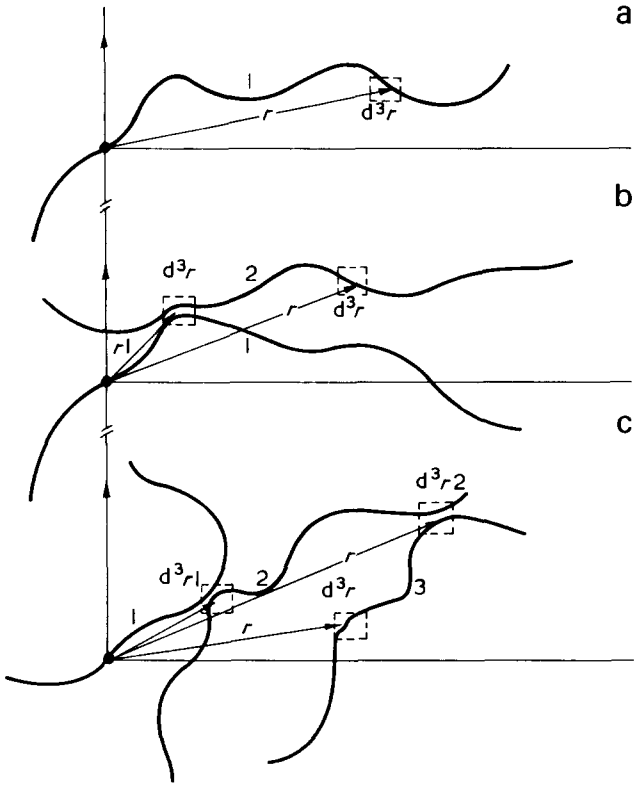

Figure 6 Schematic correlation of deuterated monomer units (CD_2) along (a) one chain; (b) two D–D chains; (c) three D–D–D chains.

Such a picture was initially interpreted in terms of a diffusion of the centre of masses of tagged molecules to form clusters with higher concentrations of tagged polymer molecules[3–5]. However, this is not the only way to account for the experimental observations. In the scattering experiments correlations between tagged monomers are observed, and these correlations can be maintained over many polymer molecules with almost no mass transport into clusters. This will be demonstrated in this section and strong arguments will be brought forward from a comparison of experimental and theoretical results to demonstrate that it is this kind of correlation which causes the paraclustering phenomena. Assuming that the fraction of D-monomer neighbours of a D-monomer unit (i.e. CD_2) is given by:

$$n_{DD} = c + (1 - c)\alpha \tag{8}$$

where c is the concentration of D-monomer units in the mixtures. Thus, n_{DD} is controlled by the parameter α such that for $\alpha = 0$ n_{DD} is the statistical value and for $\alpha > 0$ the probability of D–D monomers is enhanced. Similarly the fraction of neighbouring H-monomer units is

$$n_{DH} = (1 - c)(1 - \alpha) \tag{9}$$

and for the neighbours of H-monomer units the fractions are

$$n_{HD} = c(1 - \alpha) \text{ and } n_{HH} = (1 - c) + c\alpha \tag{10}$$

With these definitions α may be compared to the Cowley short range order parameter[16] and it follows that

$$n_{DD} + n_{DH} = 1 \text{ and } n_{HD} + n_{HH} = 1 \tag{11}$$

No other correlation between monomers of different macromolecules is taken into account in this treatment, other than nearest neighbour interactions. The correlation between the two D-monomer units occur either along one chain (which means that both D-monomers belong to the same chain), or along different chains, e.g. along two chains of type D–D, along three chains of type DDD or DHD, etc. (see *Figures 4 a–c*. According to this formalism the density $g(r)$ of D-monomer units at a distance r from a reference D-unit, assumed to be at the origin, is a sum of correlation functions, i.e.

$$g(r) = g_S(r) + g_2(r) + g_3(r) + \cdots \tag{12}$$

Here $g_S(r)$ is the correlation function between monomers belonging to the same chain whose Fourier transform is, for a Gaussian chain, the Debye function, i.e.:

$$(Z)g_S(K) = ND(K) \tag{13}$$

with $D(K) = 2/v^2(e^{-v} - 1 + v)$; $v = K^2Rg^2$

R_g is the radius of gyration and N the number of monomer units per chain. It will now be shown that the other correlation functions $g_j(r)$ can be expressed by $g_S(r)$ and α. The probability of finding a D-monomer at a distance r from a D-monomer of the same chain is $g_S(r_1)\mathrm{d}_3r_1$, the probability of finding a D-monomer of another chain in its neighbourhood of Z-neighbours is $Zn_{DD}g_S(r_1)\mathrm{d}r_1$ and the probability of finding a D-monomer of the second chain at r is

$$g_S(r - r_1)\mathrm{d}_3rZn_{DD}g_S(r_1)\mathrm{d}_3r_1$$

Therefore:

$$g_2(r) = Zn_{DD}\int g_S(r - r_1)g_S(r_1)\mathrm{d}_3r_1 \tag{14}$$

for the two chains of DD type. Its Fourier transform is

$$\tilde{g}_2(K) = Zn_{DD}\tilde{g}_S^2(K) \tag{15}$$

Similar arguments lead to

$$\tilde{g}_3(K) = Z^2n_{DD}^2\tilde{g}_3^3(K) \tag{16}$$

$$\tilde{g}_S(K) = Z^2n_{DH}n_{HD}\tilde{g}_S^3(K) \tag{17}$$

for correlations along chains of type DDD and DHD, respectively. If one proceeds according to this formalism and inserts the resulting functions into (12) the results can be written as follows:

$$\tilde{g}(K)\tilde{g}_S(K)\sum_{v=0}^{\infty}\left\{\mathfrak{N}\right\}_{11}Z^v\tilde{g}_S^v(K) \tag{18}$$

with

$$\mathfrak{N} = \begin{pmatrix} n_{DD} & n_{DD} \\ n_{HD} & n_{HH} \end{pmatrix}$$

With straightforward matrix algebra we obtain:

$$\tilde{g}(K) = \tilde{g}_S(K)\left[A^{-1}\left(\sum_{v=0}^{\infty}\tilde{g}_S{}^{v}Z^{v}\lambda_1{}^{v}\sum_{v=0}^{\infty}{}^{0}\tilde{g}_S{}^{v}Z^{v}\lambda_2{}^{v}\right)A\right]_{11} \quad (19)$$

where λ_1 and λ_2 are the eigen values of $\mathfrak{N}$ and A is defined by

$$A\,\mathfrak{N}\,A^{-1} = \begin{pmatrix}\lambda_1 & 0\\ 0 & \lambda_2\end{pmatrix}$$

Explicitly we calculate:

$$\lambda_1 = \alpha, \lambda_2 = 1 \text{ independent of } c$$

$$A = \begin{pmatrix}1 & -1\\ c & 1-c\end{pmatrix} \text{and} A^{-1} = \begin{pmatrix}1-c & 1\\ -c & 1\end{pmatrix}$$

The λ_2 sum in equation (19) is divergent for all K values of interest since $ND(K) > 1$. The sum has a finite value for a finite specimen and represents the coherent scattering of *all* monomers in the forward scattering at $K \leqslant 1/d$ where d is a specimen diameter. This scattering contribution is always present even in specimens with random distribution of scatterers and does not belong to the small-angle scattering due to correlations of D-monomers. Therefore,

$$\tilde{g}(K) = (1-c)\frac{g_S(K)}{1 - Z\alpha\tilde{g}_S(K)} \quad (20)$$

Using equation (13) the differential scattering cross-section is given by

$$\frac{d\Sigma(K)/d\Omega}{K_N M_w(1-c)c} = S(K) = \frac{D(K)}{1 - Z\alpha N D(K)} \quad (21)$$

which gives the usual relation for $\alpha = 0$ (statistical distribution).

Two approximations have been made in deriving equation (20). Firstly, any enhancement of the number of D-monomer nearest neighbours along a D-chain must be accompanied by a corresponding depletion in the number of next nearest neighbour units. Our calculations assumes a statistical distribution for next nearest neighbours, and it will be seen subsequently that for typical SANS data measured in this work ($\Sigma_0/M_w < 1000$), the pertubation from a statistical distribution is very small. Thus this approximation does not represent a serious deficiency to the theory. Secondly, the correlations between D-monomers is somewhat over-emphasized, as no account is taken of the fact that chains can come into nearest neighbour contact at more than one point. The effect of this omission is difficult to quantify, though as pointed out above, it can easily be shown that equations (20) and (21) are correct in the limit of $\alpha = 0$. Thus at $\alpha = 0$, correlations between D-monomers exist only if the monomer units belong to the same chain. For the SANS data discussed in this paper, α is typically less than or equal to 10^{-5} (see below). It therefore appears that in this region the theory is a reasonable approximation, though this need not necessarily be the case for highly clustered or partly phase segregated samples.

Using the Debye function for $D(K)$ the scattering functions $S(K)$ are plotted in a Kratky plot *versus* KR_g for various parameters $N_{cl} = \Sigma_0/M_w$ (*Figure 7*). The curves show typical features observed for the scattering pattern of clustered specimens, namely that with little clustering a constant value is rapidly reached in the Kratky plot, and that for highly clustered specimens an overshoot is observed (ref 8, *Figure 8*). Thus the paracluster model can satisfactorily describe the SANS data in the intermediate K range ($0.02 < K < 0.2$ Å^{-1}).

The degree of clustering ($N_{cl} = \Sigma_0/M_w$) is controlled by the parameter α since the enhancement of the forward scattering is $N_{cl} = (1 - ZN\alpha)^{-1}$. Simultaneously, the apparent radius of gyration $(R_g)_{app}$ deduced from the initial slope of $S(K)$ is changed from the unclustered value, R_g. We calculate

$$(R_g)^2_{app} = R_g^2 N_{cl} \quad (22)$$

Thus $(R_g)^2_{app}/R_g^2$ should be proportional to $N_{cl}{}^{1/2}$. $(R_g)^2_{app}$ and N_{cl} are the measured values for clustered samples, although R_g is not available directly. Assuming that the unclustered value of R_g is the same as the unperturbed dimensions measured in the melt and for quenched samples in the solid state[8], *Figure 8* shows a plot of $(R_g)_{app}/(R_g)$ *versus* N_{cl} for quenched, slow cooled and annealed samples on a logarithmic scale. It may be seen that a linear relation holds over three orders of magnitude, and this without any adjustable parameter. As the linear relationship is obeyed by both annealed and slow cooled (0.1°C/min) samples, this provides strong indi-

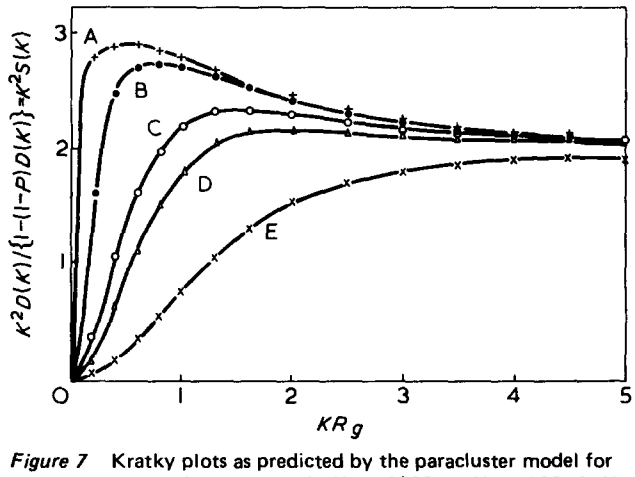

Figure 7 Kratky plots as predicted by the paracluster model for different degrees of clustering. A, $N_{cl} = 1000$; B, $N_{cl} = 100$; C, $N_{cl} = 10$; D, $N_{cl} = 5$; E, $N_{cl} = 1$

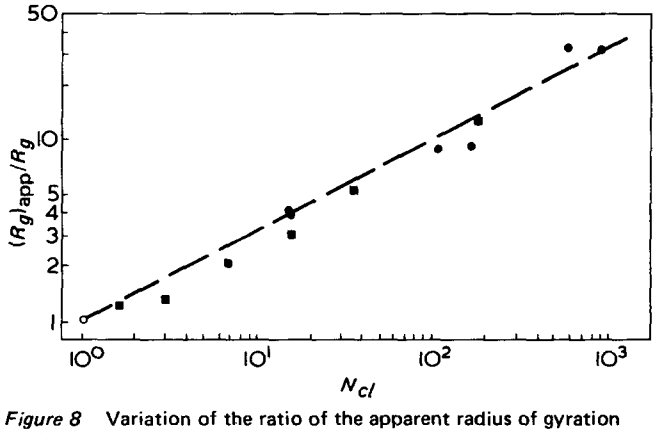

Figure 8 Variation of the ratio of the apparent radius of gyration $(R_g)_{app}$ in clustered samples, to R_g in unclustered samples, with degree of clustering N_{cl}. ○, quenched; ●, slow cooled; ■, annealed. M_w variation from 11 000–500 000. Line has a slope of 0.5 in accordance with equation (22)

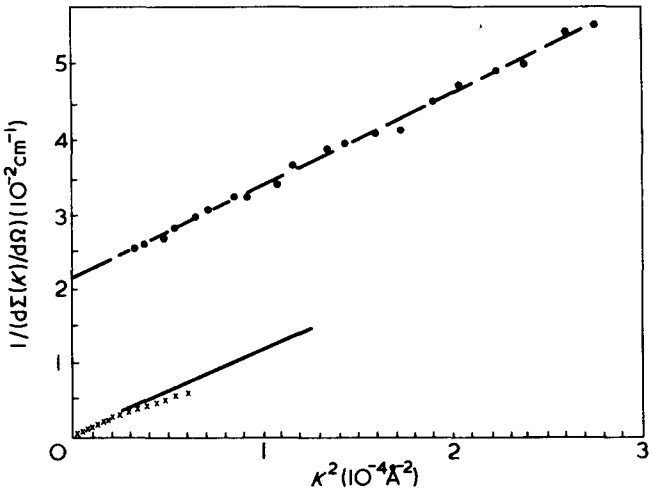

Figure 9 SANS plots in the low K region for clustered (x) and unclustered (•) molecules. M_w = 60 000, c = 5%. PE Q, $(d\Sigma/d\Omega)_0$ = 46 cm^{-1}, R_g = 134Å; PE SC, $(d\Sigma/d\Omega)_0$ = 5800 cm^{-1}, R_g = 980Å

rect evidence that on slow cooling the sample, the radius of gyration is not substantially changed from the unperturbed dimensions of the melt. In this respect polyethylene is similar to polypropylene, where direct measurements of R_g in unclustered samples lead to a similar conclusion.

In *Figure 9* the reciprocal intensities measured in a quenched (not clustered) and a slow cooled (heavily clustered) specimen are shown *versus* K^2 in the low K range ($K < 0.02$ Å^{-1}). It may be seen that in both cases the data points follow straight lines. In addition the straight line have the same slopes (see also *Figure 4*). These observations are quite in accordance with our model. From equation (21) we obtain

$$1/S(K) = 1/D(K) - ZN\alpha \qquad (23)$$

For the Debye function it is known that in this region

$$D(K)^{-1} = 1 + {}^1/_3K^2R_g{}^2$$

holds to a good approximation. Inserting this into equation (23) gives

$$S^{-1}(K) = (1 - ZN\alpha) + {}^1/_3K^2R_g^2$$

i.e. according to our theory the effect of clustering is merely a parallel shift of the curves $S^{-1}(K)$ *versus* K^2 as observed experimentally (*Figures 4 and 9*).

For large K values $S(K)$ approaches $D(K)$ i.e. the scattering from a clustered specimen can be predicted to be the same as that of a specimen in which the tagged molecules are statistically distributed. From *Figure 7* we see that there is less than 10% difference between all curves for $KR_g \geqslant 4$. This is in complete accordance with the experimental findings that all scattering curves had the same tail irrespectively of their degree of clustering[8].

The molecular weight dependence of $N_{cl} = (1 - \alpha NZ)^{-1}$ is shown in *Figure 10* for polyethylene specimens which were quenched, annealed and slow cooled (*Table 5*). There is a common tendency in the data for N_{cl} to increase with decreasing molecular weight. Thus αNZ becomes closer to unity as N decreases, though for an equilibrium distribution one would expect the opposite behaviour. This confirms our assumption that the nearest neighbour distribution does not represent the equilibrium state (α independent N) for para-clustered samples, and that the mobility of the molecules is also an important factor in producing non-statistical distribution.

In summary, there are strong arguments that the para-clustering phenomena are caused by correlations between D-monomer nearest neighbours, and this concept explains all the general features of the SANS data. These correlations come about because of the tendency of tagged molecules to aggregate, due to the thermodynamic driving forces described above.

DISCUSSION

In the previous section arguments were presented in favour of a new way of interpreting experimental SANS data concerning clustering phenomena. In this section consequences from this new model will be discussed. Since in equation (21) $ZN\alpha$ is limited to unity and for high molecular weight polymers $N \geqslant 1000$ and $Z \geqslant 4$, we obtain very small Cowley[16] parameter values. Thus, the fraction of D-monomer neighbours of a deuterated chain is only slightly larger with respect to the fraction for statistical distribution. The factor N in αNZ arises from the fact that a correlation between two D-monomers of different chains is built up if for any D-monomer along chain 1 it is known that there is a D-monomer

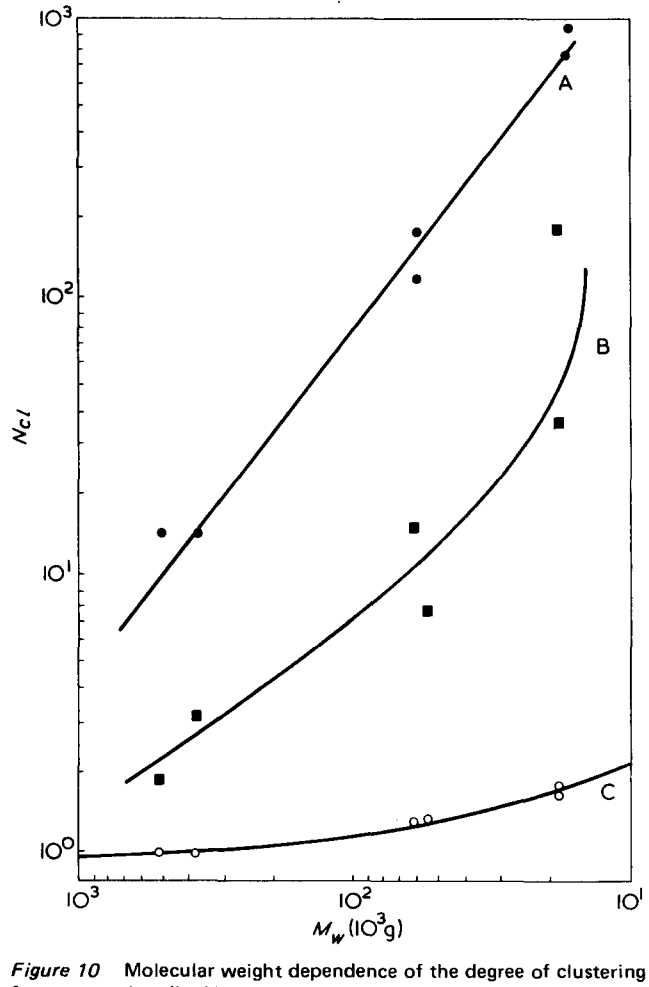

Figure 10 Molecular weight dependence of the degree of clustering for samples described in *Table 5:* A, slow cooled; B, annealed; C, quenched

of another chain in its neighbourhood. Because of this large factor N, very small values of α can cause large scattering values in the forward direction.

In order to estimate how far the D-monomer units were displaced from their positions at random distribution in order to establish the observed non-random distribution, let us assume that the enhancement of the forward scattering is $N_{cl} = \Sigma_0/M_w = 100$, in a specimen of polymers of molecular weight of $M_w = 150\,000$, equivalent to $N = 10\,000$, and that the concentration of tagged molecules is $c = 3\%$. For $Z = 4$ the total number of monomer neighbours is 40 000 for a tagged polymer molecule. From these, 1201 neighbours are D-monomers instead of 1200 as it would be for random distribution. The mean distance between D-monomers of different chain is $\simeq 25$Å for $c = 3\%$. Thus displacements much smaller than 25Å are sufficient to cause the strong deviation of the scattering curve with respect to that for statistical distribution. It may be surprising at first sight that such small deviations are sufficient to cause such strong effects in the scattering curve. However two chains of tagged molecules would have to systematically come into contact at only one point along the chains, for the molecules to diffract as one molecule with twice the individual molecular weight. As this point of contact need involve only a few of the thousands of monomer units, the above conclusions are given some plausibility, and indicate how the apparent molecular weight can be changed to many times its true value, with almost no mass transport of the chain. It appears therefore that neutron scattering is an extremely sensitive method of detecting these very minor changes from a statistical distribution, and that for typical values of the degree of clustering $1 < N_{cl} < 1000$ the statistical distribution is only slightly perturbed.

We had earlier pointed out that the clustering phenomenon could have important implications for recent i.r. studies of chain conformation in PEH/PED mixtures[11–13]. Bank and Krimm[12] used experimental i.r. studies of mixed crystals of PEH and PED to distinguish between chain folding with adjacent re-entry and random re-entry. Basing their interpretation on the earlier work of Tasumi and Krimm, they concluded that folding occurred with adjacent re-entry for both dilute solution grown material and melt crystallized polymer. Subsequently there was discussion in the literature as to whether differences in the concentration of tagged molecules (PED) for crystals formed at different stages of crystallization could affect this conclusion[10,13]. Setting aside this question, our model clearly points to another factor which may affect the conclusion, i.e. the possibility that there is a non-statistical distribution of PED molecules in the crystal, irrespective of variations in the overall PED concentration, c. We can now predict that for small degrees of clustering ($1 < N_{cl} < 100$) the i.r. data will be completely unaffected by clustering as the distribution of neighbours of the molecules is virtually statistical, and the system is in no physical sense aggregated. Thus for samples prepared with a relatively rapid cooling from the melt, or with low mobility (high molecular weight) of the tagged and matrix molecules, clustering will cause little effect on the i.r. data. Only the extreme sensitivity of the SANS technique allows such tiny departures from a statistical distribution to cause such a strong effect in the SANS data.

However, the thermodynamic considerations outlined above show that under appropriate non-equilibrium crystallization the distribution of PED in PEH is almost completely phase separated, and hence for samples crystallized very slowly ($\simeq 1^\circ$C/min), with high molecular mobility, the i.r. data will be strongly perturbed by aggregation effects. This aggregation will progress far beyond the paracluster stage to virtually complete phase segregation. Thus it is recommended that in future the data given above be used to plan i.r. measurements, and to ensure that the degree of clustering is kept small ($N_{cl} < 100$), where the i.r. data is virtually unaffected. Preferably a check on the degree of clustering should also be made by SANS methods.

REFERENCES

1 Kirste, R. G., Kruse, W. A. and Schelten, J. *Makromol. Chem.* 1972, **162**, 299; Ballard, D. G. H., Schelten, J. and Wignall, G. D. 'Symposium on Molecular Weight Characterization of Industrial Polymers National Physical Laboratory', (Eds J. H. S. Green and R. Dietz), Transcripta, London, 1973; *Eur. Polym. J.* 1973, **9**, 965, Benoit, H., Cotton, J. P., Decker, D., Farnoux, B., Higgins, J. S., Jannink, G., Ober, R. and Picot, C. *Nature* 1973, **245**, 13

2 Wignall, G. D., Ballard, D. G. H. and Schelten, J. *Eur. Polym. J.* 1974, **10**, 861

3 Schelten, J., Wignall, G. D. and Ballard, D. G. H. *Polymer* 1974, **15**, 682

4 Schelten, J., Wignall, G. D., Ballard, D. G. H. and Schmatz, W. *Colloid Polym. Sci.* 1974, **252**, 749

5 Wignall, G. D., Ballard, D. G. H. and Schelten, J. *J. Appl. Phys. (B)* 1976, **12**, 75

6 Lieser, G., Fischer, E. W. and Ibel, K. *J. Polym. Sci.* 1975

7 Sadler, D. M. and Keller, A. A. *Polymer* 1976, **17**, 37

8 Schelten, J., Ballard, D. G. H., Wignall, G. D., Longman, G. W. and Schmatz, W. *Polymer* 1976, **17**, 751

9 Kruse, W. A., Kirste, R. G., Haas, J., Schmitt, B. J. and Stein, D. J. *Makromol. Chem.* 1976, **177**, 1145

10 Stehling, F. S., Ergos, E. and Mandelkern, L. *Macromolecules* 1971, **4**, 672

11 Tasumi, M. and Krimm, J. *J. Polym. Sci. (A-2)* 1968, **6**, 995

12 Bank, M. I. and Krimm, S. *J. Polym. Sci. (A-2)* 1969, **7**, 1785

13 Krimm, S. and Ching, J. H. C. *Macromolecules* 1972, **5**, 209

14 Denbigh, K. 'Principles of Chemical Equilibrium', Cambridge University Press, Cambridge, 1961, p 289

15 Brandrup, J. and Immergut, E. H. 'Polymer Handbook' Interscience, New York, 1969, p III-5

16 Cowley, J. M. *J. Appl. Phys.* 1959, **21**, 24